SECOND-ORDER LUGRE FRICTION MODEL

Acho L., Moreno J., and Guerra R.
CITEDI – IPN
Av. del Parque No. 131º, Mesa de Otay, Tijuana, Baja California,
México C.P. 22510
leonardo@citedi.mx
rguerra@citedi.mx

ABSTRACT
A second-order LuGre friction model is presented which can be viewed as an extension of the well known LuGre friction model. This model is based on a dynamic extension, which can be seen as an extra dynamic to capture some kind of periodic motion produced by the bristles in motion. The additional dynamic can be viewed as an internal disturbance due to the vibration associated with the use of motors. Our model can capture the friction phenomena of the original LuGre friction model and presents two new behaviors, one is the multi-loop behavior in the hysteresis curve when velocity is varied during unidirectional motion, and the other, in the pre-sliding motion curve of friction force versus displacement in the spring regime, where two jumps appear.

KEY WORDS
Friction, friction model, hysteresis.

1.Introduction

Friction modeling is an important issue in control theory because, in most cases, the design of a control law is based on the model of the plant to be controlled. In this context, a congruent friction model that captures all the phenomena that the friction produces in a mechanical system, such as: stribeck effect, pre-sliding motion, hysteresis, etc., is highly important. So far, there exist three important friction models: 1) The Coulomb model, 2) The Dahl model, and 3) The LuGre model. The first one is a static model whereas the others are dynamical. It is well know that dynamical models can produce most of the phenomena produced by friction [1]. There have been some techniques to compensate friction forces, see for example [2]-[4]. For instance, in [2] the Coulomb friction model is used for the compensator design; however, and as it is pointed out in [2], if this model differs from reality, this techniques is not effective. In [5] a chattering control design is presented to uncouple the effects of the friction forces on the mechanical system, but, it requires a control law that commutes very fast, which is hard to produce because of the high band required to drive the control-law's signal. The demonstration of this important fact was possible using the LuGre friction model. In this work (in [5]), it is also shown that the chattering control law is robust against variation in the friction model used; in other words, in the simulation experiments shown in [5], with Dahl model or LuGre model, the chattering control law could uncouple the effects of the friction forces on the system.

One important observation on friction model is that this is not unique, that is, there can exist other friction models that can captures most of the phenomenon produced by friction force. The main objective of the present paper is to show that there exists a modification of the LuGre friction model (a second order model) that can still capture the main effects of friction force; however two other effects appears, for instance, the Hysteresis effect which is produced when velocity is varied during unidirectional motion, in our model, presents multi-loop variation which is not captured by the LuGre model. Also, the pre-sliding motion curve of friction force versus displacement in the spring regime, presents a jump, which is not captured by LuGre model. This jump appears in experimental and simulations results shown in [6]. Other friction models have been reported recently (see [6], [7], and [8]), our model differs from them by the fact that we are using an extra nonlinear dynamic to capture some kind of periodic motion produced the average deflection of the moving elastic bristles, this additional dynamic can be attributed to an internal disturbance, such as the vibration generated by motors intended to produce motion.

II. LuGre Friction Model

The LuGre friction model is given by [1]:

$$\begin{aligned} \dot{z} &= \frac{dz}{dt} = v - \frac{|v|}{g(v)} z \\ F &= \sigma_0 z + \sigma_1 \dot{z} + \sigma_2 v \\ \sigma_0 g(v) &= F_C + (F_S - F_C) e^{-(v/v_S)^2} \end{aligned} \tag{1}$$

where v is the relative velocity between the surfaces in contact that produce friction, z denotes the average deflection of the bristles, F is the friction force, σ_0 is the stiffness, σ_1 is the damping coefficient, σ_2 is the viscous coefficient, F_C is the Coulomb friction level, F_s is the level of the stiction force, and v_s is the Stribeck velocity.

The LuGre friction model is a first-order model and it depends on the internal state $z(t)$. However, it is still possible to produce a new friction model that can capture the natural phenomena produced by friction. This model can be viewed as a second-order LuGre friction model:

$$\dot{z} = \frac{dz}{dt} = v - \frac{|v|}{g(v)} z$$
$$\dot{w} = v - f(w);\ f(w) = \frac{w^3}{\alpha} - w$$
$$F = \sigma_0 z + \sigma_1 \dot{z} + \sigma_2 (v + \beta w)$$
$$\sigma_0 g(v) = F_C + (F_S - F_C) e^{-(v/v_S)^2} \qquad (2)$$

where α and β are two constant parameters.

The extra dynamic added was proposed to capture some kind of periodic motion produced by the bristles in movement, in fact, the nonlinear function $f(w)$ is common in nonlinear oscillator and this is the special case for the Van der Pol oscillator (see [9] page 427). So, the constants α and β can be interpreted as the size of the active region (definition used in nonlinear oscillator) of $f(w)$ (see section *IV* too) and amplitude gain, respectively. This last one is justified because it appears as a gain in the friction force F in (2). Obviously, these constants need some technical specifications that can be done with experimental correlation, which are not presented here.

The physical justification for extending the friction model to a second order system is to account for internal vibration, an occurrence common in mechanical systems that rely on motors. When the motor is active, the microscopic gaps in the mechanical assembly generate vibration in addition to the intended motion; this can be viewed as an internal disturbance that alters the behavior of the system.

The friction model given in (2) has the following property:

Property 1: Assume that $0<g(v)\leq a$ then $|z(t)| \leq a$ for all $t>0$ and $w(t)\in L_\infty$.

Proof: The first part of the property is proved in [1]. Because the proof given in [1] is trough a Lyapunov function that depends on $v(t)$, then $v(t)\in L_\infty$. Using the fact that there exist a positive constant b such that $|v(t)| \leq b$ for all $t>0$, and using $V=w^2/2$, the time derivative of V evaluated along of the solution of $w(t)$ is

$$\dot{V} = w[v - f(w)] \leq w[b - f(w)]$$
$$= w^2[\frac{b}{w} - \frac{f(w)}{w}];\ w \neq 0\ (with\ w = 0 \Rightarrow \dot{V} = 0)$$

when $w\neq 0$, $\dot{V}$ is negative semi-definite if

$$\frac{b}{w} - \frac{f(w)}{w} < 0\ or$$
$$b < f(w) = \frac{w^3}{\alpha} - w < |w|\left[\frac{|w|^2}{\alpha} - 1\right] \leq \frac{|w|^3}{\alpha} \Rightarrow |w| \geq (b\alpha)^{1/3}$$

The above equation says that the solution $w(t)$ can not leave a compact set. If $w(0)$ is beyond to this set, then trajectory $w(t)$ converges asymptotically to this set, and after that, this trajectory can no leave this set, which means that $w(t)\in L_\infty$.

III. Dynamical Behavior

In this section we produced numerical experiments to show that the friction model (2) captures most of the phenomenon that friction force produces in a given system. In all our simulations, we used the parameters given in Table I ([1]).

A. *Limit Cycles Produced by Friction*

To illustrate that friction can produce limit cycles in a mechanical system, we consider the same experiment used in [1]; *i.e.*, we consider a mass m in contact with a horizontal surface (see Fig. 1):

$$m\frac{d^2x}{dt^2} = u - F \qquad (3)$$

where $x(t)$ is the position, $\dot{x}(t) = v(t)$ is the velocity, F is the friction force and u is the control input. Consider the following PID controller [1]:

$$u = -k_v v - k_p(x - x_d) - k_i \int (x - x_d) d\tau$$
(4)

where x_d is the desired position or set-point. Using $k_p=3$, $k_i=4$, $k_v=6$, $m=1$, and $x_d=1$, the simulation results are shown in Fig. 2.

B. *Stick-Slip Motion*

Employing the same experiment presented in [1], we used the experimental set up shown in Fig. 3 with unit mass. The experiment consists of attaching a spring with stiffness $k=2N/m$ to the block and the end of the spring was pulled with constant velocity; *i.e*, $dy/dt=0.1m/s$. Fig.

4 shows the simulation results. This experiment reproduced the stick-slip motion caused by friction.

TABLE I
PARAMETERS VALUES USED.

Parameter	Value	Unit
σ_0	10^5	*N/m*
σ_1	$\sqrt{10^5}$	*Ns/m*
σ_2	*0.4*	*Ns/m*
F_C	*1*	*N*
F_S	*1.5*	*N*
v_s	*0.001*	*m/s*
$\propto$	*3*	
β	*1*	

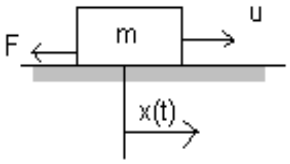

Fig. 1 Experimental system.

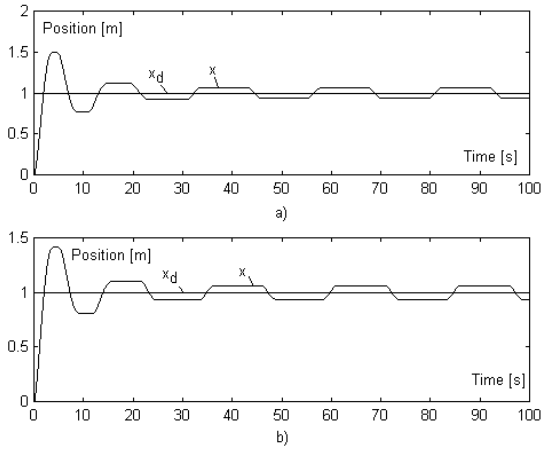

Fig. 2 Simulation of the PID control law:
a) Using model (1), b) Using model (2).

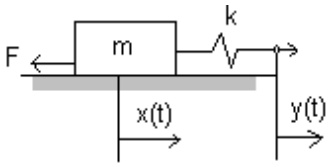

Fig. 3 Experimental sep-up.

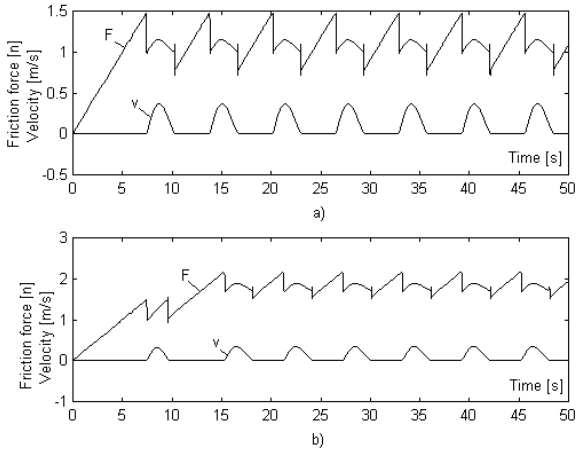

Fig. 4 Simulation of the stick-slip motion:
a) Using model (1), b) Using model (2).

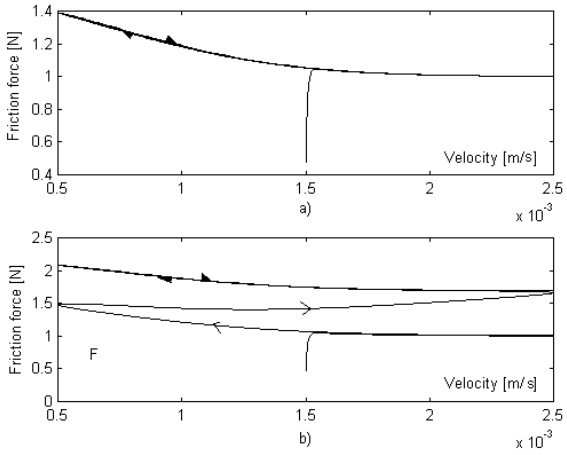

Fig. 5 Simulation of the Hysteresis effect when 2π *f=1rad/s*:
a) Using model (1),
b) Using model (2).

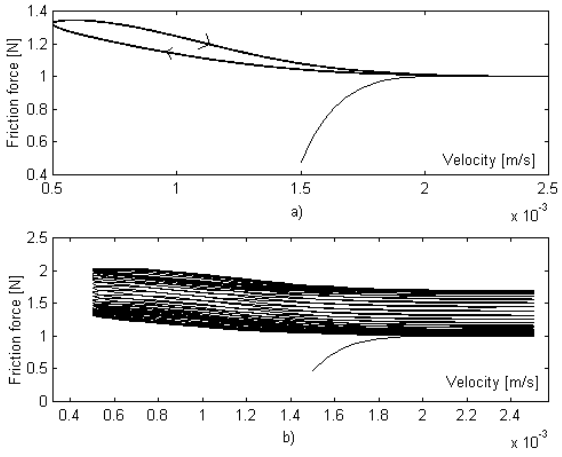

Fig. 6 Simulation of the Hysteresis effect when $2\pi f = 25 rad/s$: a) Using model (1), b) Using model (2).

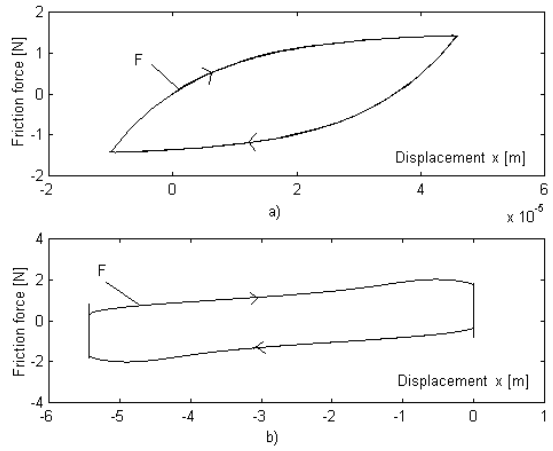

Fig. 7 Simulation of the Pre-sliding effect: a) Using model (1), b) Using model (2).

C. Frictional Lag

The effect of frictional lag can be viewed by applying a sinusoidal velocity to the input of the friction model. This sinusoidal variation is around an equilibrium or DC component. Simulation results are shown in Figure 5 and Figure 6 for *1 rad/s* and *25 rad/s* respectively. Observe the multi-loop behavior in our model.

D. Pre-sling Displacement

The pre-sliding displacement can be captured by applying a force that varies slowly ramped up to 1.425 N, and after kept constant for a while, and later ramped down to -1.425 N, where, again, it is kept constant for a while and then again ramped up to 1.425 and so on (see [1]). Simulation results are shown in Fig. 7. Figure 7 b) shows a constant force while displacement is zero (the vertical lines). This behavior is not captured by model (1). In Fig 7 b), the displacement is bigger that in Fig. 7 a); however, this can be manipulated by changing the parameters β and α. Observe the presences of two jumps in our model. These jumps were observed in [8] too.

IV. Remark

In model (2), *f(w)* has the following properties:

1) *f(0)=0*
2) *f'(0)<0*
3) *f(w) tends to $+\infty$ as w tends to $+\infty$*
4) *f(w) tends to $-\infty$ as w tends to $-\infty$*

The above means that it is possible to replace *f(w)* by other non-linear function that satisfies these properties. The contribution of parameter α can be viewed as the boundary of the active region that satisfies $wf(w)<0$ and $f'(w)\leq 0$ (see Fig. 8).

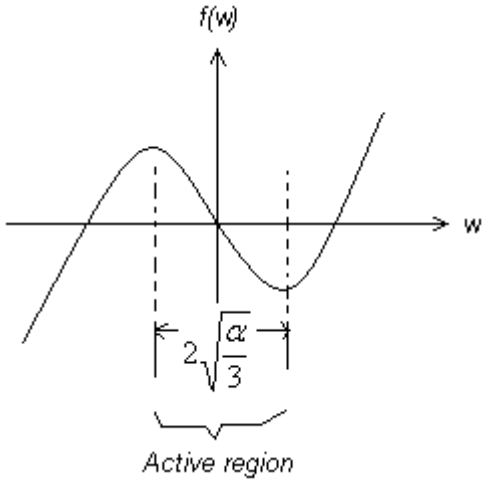

Fig. 8 Nonlinear function *f(w)*.

In model (2), *w(t)* can be interpreted as a complement of the average dynamic *z(t)*. For instance, consider that *v* is constant and for simplicity assume that *v=0*. Then $\dot{w} = -f(w)$ has its origin a repulsive system being the region of repulsion the active region. This repulsion is translated into force in (2) and it can be the reposition force of the bristles in motion.

An additional discussion about Figure 4 b) with respect to the "stick-slip" behavior during the 15 seconds of the simulation experiments can be stated as follows. This "stick-slip" motion can be interpreted as an induced dynamic "Stribeck" effect on the system.

References:

[1] C. Canudas de Wit, H. Olsson, K. J. Astrom, y P. Lischinsky, "A new model for control of systems with friction", *IEEE Trans. Aut. Ctrl.*, Vol. 40, No. 3, 1995. 419-425.

[2] B. Friedland y Y.-J. Park, "On adaptive friction compensation", *IEEE Trans. Aut. Ctrl.*, Vol. 37, No. 10, 1992. 1609-1612.

[3] Liao T.y Chien T., "An exponentially stable adaptive friction compensator", *IEEE Trans. Aut. Ctrl*., Vol. 45, No. 5, 2000. 977-980..

[4] Zhang T., y Guag M., "Commnets on 'An exponential stable adaptive friction compesator'", *IEEE Trans. Aut. Ctrl.*, Vol. 46, No. 11, 2001. 1844-1845.

[5] Acho L., "On PID chattering control law to cope with friction forces", *Procc. IASTED Int. Conf., Circuits, Signals, and Systems*, Cancún, México, 2003.

[6] Swevers J., Al-Bender F., Ganseman C. G., and Tutuko Prajogo, "An integral friction model structure with improved pre-sliding behavior for accurate friction compensation", IEEE Trans. on Aut. Control, Vol. 45, No. 4, 2000, 675-686.

[7] Lampaert V., Swevers J., and Al-Bender-Al, "Modification of the Leuven integrated fricition model structure", IEEE Trans. on Aut. Control, Vol. 47, No. 4, 2002, 683-687.

[8] Dupont P., Hayward V., Armstrong B., and Altpeter F., "Single state elastoplastic friction models", IEEE Trans. on Aut. Control, Vol. 47, No. 5, 2002. 787-792.

[9] Chua L. O., Desoer C. A., and Kuh E. S, *Linear and nonlinear circuits*, Prentice Hall, Singapore, 1987.